The Mechanism of Heme Transfer from the Cytoplasmic Heme Binding Protein PhuS to the δ-Regioselective Heme Oxygenase of *Pseudomonas aeruginosa*†

Mehul N. Bhakta and Angela Wilks*

Department of Pharmaceutical Sciences, School of Pharmacy, University of Maryland, 20 Penn Street, Baltimore, Maryland 21201

Received May 17, 2006; Revised Manuscript Received July 14, 2006

ABSTRACT: The opportunistic pathogen *Pseudomonas aeruginosa* has evolved two outer membrane receptor-mediated uptake systems (encoded by the *phu* and *has* operons) by which it can utilize the hosts heme and hemeproteins as a source of iron. PhuS is a cytoplasmic heme binding protein encoded within the *phu* operon and has previously been shown to function in the trafficking of heme to the iron-regulated heme oxygenase (*pa*-HO). While the heme association rate for PhuS was similar to that of myoglobin, a markedly higher rate of heme dissociation ($\sim 10^5$ s^{-1}) was observed, in keeping with a function in heme-trafficking. Additionally, the transfer of heme from PhuS to *pa*-HO was shown to be specific and unidirectional when compared to transfer to the non-iron regulated heme oxygenase (BphO), in which heme distribution between the two proteins merely reflects their relative intrinsic affinities for heme. Furthermore, the rate of transfer of heme from holo-PhuS to *pa*-HO of 0.11 ± 0.01 s^{-1} is 30-fold faster than that to apo-myoglobin, despite the significant higher binding affinity of apo-myoglobin for heme ($k_H = 1.3 \times 10^{-8}$ μM) than that of PhuS (0.2 μM). This data suggests that heme transfer to *pa*-HO is independent of heme affinity and is consistent with temperature dependence studies which indicate the reaction is driven by a negative entropic contribution, typical of an ordered transition state, and supports the notion that heme transfer from PhuS to *pa*-HO is mediated via a specific protein−protein interaction. In addition, pH studies, and reactions conducted in the presence of cyanide, suggest the involvement of spin transition during the heme transfer process, whereby the heme undergoes spin change from 6-c LS to 6-c HS either in PhuS or *pa*-HO. On the basis of the magnitudes of the activation parameters obtained in the presence of cyanide, whereby both complexes are maintained in a 6-c LS state, and the biphasic kinetics of heme transfer from holo-PhuS to *pa*-HO-wt, supports the notion that the spin-state crossover occur within holo-PhuS prior to the heme transfer step. Alternatively, the lack of the biphasic kinetic with *pa*-HO-G125V, 6-c LS, and with comparable rate of heme transfer as *pa*-HO is supportive of a mechanism in which the spin-change could occur within *pa*-HO. The present data suggests either or both of the two pathways proposed for heme transfer may occur under the present experimental conditions. The dissection of which pathway is physiologically relevant is the focus of ongoing studies.

Heme, a cofactor of proteins involved in a variety of biological processes such as oxygen transport and storage, oxygenation reactions, electron transfer, and transcriptional regulation is also a redox-reactive, hydrophobic iron chelate that readily associates with membranes and is toxic to cells due to its ability to generate reactive oxygen species. Therefore, aerobic organisms have developed strategies to protect themselves from the harmful effects of "free" heme by sequestering it within specific proteins (*1*, *2*). While hemeproteins serve a variety of biological functions, very little is understood on the transport and shuttling of heme within cells. Furthermore, heme has been shown to be a source of iron in numerous pathogenic bacteria and is required for survival and virulence (*1*, *2*). Bacterial pathogens have developed sophisticated mechanisms by which they acquire heme directly from the host's hemeproteins or via a secreted hemophore that sequesters and returns heme to the outer-membrane receptor for internalization and further utilization (*3*−*8*). Once internalized, heme is degraded by soluble heme oxygenases to biliverdin, CO, and free iron, and whereas the overall mechanism of heme degradation by bacterial HOs is fairly well-understood (*9*), very little is known on how heme is transported within the bacterial cell.

The opportunistic pathogen *Pseudomonas aeruginosa*, a Gram-negative bacterium, causes infections of immune-compromised individuals, specifically cystic fibrosis patients and burn victims (*10*−*12*). In addition *P. aeruginosa* is rapidly becoming a leading cause of nosocomial infections in hospital and community settings. *P. aeruginosa* encodes two iron-regulated heme uptake operons, the *Pseudomonas* heme utilization (*phu*)[1] and heme assimilation system (*has*) (*7*). The *phu* operon encodes an outer membrane receptor (PhuR) and the cytoplasmic ATP-ase and permease proteins (Phu U and V) which comprise an ABC-transporter required

* Address correspondence to Angela Wilks, Department of Pharmaceutical Sciences, School of Pharmacy, University of Maryland, 20 Penn Street, Baltimore, Maryland 21201. Tel., 410 706-2537; fax, 410 706-5017; e-mail, awilks@rx.umaryland.edu.

† This work was supported by National Institutes of Health Grant AI-48551.

10.1021/bi060980l CCC: $33.50
Published on Web 09/02/2006

for internalization of the heme. In addition, the *phu* operon encodes a periplasmic-binding protein (PhuT) a soluble receptor for the ABC transporter, and a cytoplasmic binding protein (PhuS) whose function is not well-understood (*7*). In contrast, the *has* operon encodes the outer-membrane receptor (HasR), a secreted hemophore (HasA), and the ATP-ase/permease (HasU and V) required for secretion of the hemophore (*13*). While many of the proteins have either been characterized or have proposed functions based on similarity to the well-characterized iron-siderophore uptake proteins, the cytoplasmic heme binding protein (PhuS) were proposed to be heme oxygenases. This hypothesis was based on early genetic studies in which the *phuS* gene homologue *hemS* of *Yersinia entercolitica* on deletion showed heme toxicity when heme was given as the sole source of iron (*14*). We have recently characterized the heme binding protein, PhuS, in *P. aeruginosa* as a heme-chaperone to the previously characterized iron-regulated heme oxygenase, *pa*-HO (*15*). More recently a second heme oxygenase BphO was characterized, and in contrast to *pa*-HO, it is not iron-regulated and yields biliverdin IXα as the product of the reaction, and not the δ-regioselective isomer as for *pa*-HO. The α-biliverdin chromophore is transferred to the receptor protein (BphP) of a two-component sensor kinase for which the downstream function remains unknown (*16, 17*). These recent findings further confirmed the role of the iron-regulated *pa*-HO is solely in the mining of iron, suggesting that transfer of heme from PhuS is specific to the iron-regulated *pa*-HO.

Initial spectroscopic characterization of the heme-PhuS complex at neutral pH indicates the heme to be predominantly six-coordinate low spin (6-c LS) (*15*). However, heme-*pa*-HO at neutral pH has a six-coordinate high spin (6-c HS) heme; therefore, we hypothesize that heme transfer from PhuS to *pa*-HO involves a switch in both the axial heme ligand and a change in the heme spin-state. In the present study, we have further characterized PhuS as a specific heme transfer protein to *pa*-HO based on competitive studies carried out with *pa*-HO, selected *pa*-HO-mutants with either an altered heme seating or spin-state, BphO the non-iron regulated HO, myoglobin, and bovine serum albumin (BSA). In addition, the mechanism of heme transfer from PhuS to *pa*-HO was investigated by measuring the kinetics of this process at several temperatures in the presence and absence of CN^- in order to provide a better understanding of the heme transfer pathway. Taken together, the data indicates that PhuS transfers heme specifically to *pa*-HO, and a switch in spin-state from low-spin to high-spin occurs either in PhuS or *pa*-HO during the heme transfer.

MATERIALS AND METHODS

Materials. Hemin, myoglobin, and bovine serum albumin (BSA) were purchased from Sigma-Aldrich. All other chemicals and reagents purchased were ACS reagent grade or higher. Heme solutions were prepared by dissolving heme in 0.1 N sodium hydroxide and buffering with 20 mM Tris (pH 7.5) unless otherwise stated. Cyanoferric complexes of holo-PhuS and holo *pa*-HO were generated by the addition of excess amount of KCN (10 mM) [Caution: Addition of acid to solutions containing cyanide can generate poisonous HCN gas].

Purification and Preparation of Proteins. Apomyoglobin was prepared using the methyl ethyl ketone method described by Ascoli et al. (*18*). After hemin extraction with methyl ethyl ketone at acidic pH, apoglobin was dialyzed extensively against 20 mM Tris, pH 7.5. The apoprotein was then centrifuged to remove any remaining precipitate and concentrated to approximately 0.5 mM using an ϵ_{280} of 15.2 mM^{-1} cm^{-1} and stored at −80 °C. The PhuS, *pa*-HO-wt, *pa*-HO-mutants, and BphO proteins were expressed and purified as described previously (*15, 19*).

Heme Transfer Experiments. All heme transfer kinetic experiments were carried out with an Applied Photophysic stopped flow spectrometer (model SX.18MV) unless otherwise stated. Sample preparation was carried out as previously reported (*15*). In brief, components of the reactions were mixed and preincubated for 5 min at the appropriate temperature. Heme transfer studies were conducted in the presence 10 μM PhuS and 30 μM *pa*-HO in 20 mM Tris, pH 7.5, unless otherwise stated and were monitored at 405 and 419 nm in the absence and presence of 10 mM CN^-, respectively.

Heme transfer experiments from holo-PhuS to apo *pa*-HO, apomyoglobin, or BSA were followed by UV−visible spectrometry, and full spectra were collected as a function of time. The absorbance changes at the appropriate wavelength were fitted to either a one- (eq 1) or a two-exponential decay (eq 2) where k_1 and k_2 are the observed rate constants for the fast and slow phases, respectively. A_1 and A_2 are related to the initial absorbances, and A_t is the absorbance at time t. The calculated k_{obs} values for each reaction were determined from the average of at least three measurements. Nonlinear curve fitting of the data was performed with the supplied Applied Photophysics software and Sigma-Plot. The

$$A_t = A_0 + A_1(1 - e^{-k_1 t}) \quad (1)$$

$$A_t = A_0 + A_1(1 - e^{-k_1 t}) + A_2(1 - e^{-k_2 t}) \quad (2)$$

extent of heme transfer from the heme−PhuS complex to *pa*-HO, BphO, and BSA was verified by UV−visible absorbance (406 nm for heme, 280 nm for protein) and SDS−PAGE analysis of chromatographic fractions separated from the reaction mixture by gel filtration (Sepharose S-100, 1.5 × 120-cm column, equilibrated with 20 mM Tris-HCl (pH 8.0), 100 mM NaCl).

Temperature-Dependence Analysis. The natural log of the rate constants for each averaged set of experimental data were plotted against the reciprocal of the absolute temperature. The data were then fit to the Arrhenius equation (eq 3) using the linear fitting function in the plotting program sigma plot. In this equation, A is the Arrhenius pre-exponential factor and R is the gas constant. The activation enthalpy and activation entropy and Gibbs free energy of heme transfer

[1] Abbreviations: *pa*-HO, *Pseudomonas aeruginosa* δ-regioselective heme oxygenase; BphO, *Pseudomonas aeruginosa* α-regioselective heme oxygenase; CN^-, potassium cyanide solution, heme, protoporphyrin IX regardless of oxidation state; *has*, heme assimilation system; *phu*, *Pseudomonas* heme uptake; 6-c HS, six-coordinate high spin; 6-c LS, six-coordinate low spin.

Table 1: Kinetic and Equilibrium Parameters for Heme Binding to Various Hemeproteins

protein	k_H (M^{-1} s^{-1})	k_{-H} (s^{-1})	K_d (M)
Myoglobin[a]	7.0×10^7	8.4×10^{-7}	1.3×10^{-14}
BSA[b]	5.0×10^4	3.2×10^{-4}	6.4×10^{-9}
pa-HO	1.1×10^5 [c]	6.6×10^{-2}	0.6×10^{-6} [d]
PhuS	1.8×10^5 [c]	3.6×10^{-2}	0.2×10^{-6} [d]

[a] Values reported by Hargrove et al. (*21*), for the binding of Fe−CO to apomyoglobin. [b] Reported by Gattoni et al. (*20*), binding of free heme to apoalbumin. [c] All association rate constants (k_H) were measured using heme in 20 mM Tris-HCl, pH 8.0, at 25 °C. The dissociation rate constants (k_{-H}) were calculated from K_d, which is the ratio of k_{-H}/k_H. [d] K_d was obtained by fluorescence quenching and UV−vis spectroscopy and is an estimate of heme affinity for the apoprotein sample.

were determined using eqs 4, 5, and 6, respectively, where k_B is the Boltzmann constant and $\hbar$ is Planck's constant.

$$\mathrm{Ln}\, k = \ln A - E_a/RT \quad (3)$$

$$\Delta H^{\ddagger} = E_a - RT \quad (4)$$

$$\Delta S^{\ddagger} = R(\ln A - \ln(k_B T/\hbar)) \quad (5)$$

$$\Delta G^{\ddagger} = \Delta H^{\ddagger} - T\Delta S^{\ddagger} \quad (6)$$

RESULTS

Heme Binding to PhuS and pa-HO. We have previously shown that both PhuS and *pa*-HO bind one heme per monomer with similar affinities of 0.6 and 0.2 μM for *pa*-HO and PhuS, respectively (*15*). The kinetics of the reactions were investigated by mixing 2 μM heme with either PhuS or *pa*-HO in a stopped-flow apparatus at concentrations between 20 and 100 μM of apoprotein, and monitored at either 410 or 405 nm, respectively. Heme solutions were used at a low concentration to minimize the tendency to form μ-oxo-dimers. As shown in Table 1, association rate constants of $(1.8 \pm 0.1) \times 10^5$ and $(1.1 \pm 0.1) \times 10^5$ M^{-1} s^{-1} were obtained for heme binding to PhuS or *pa*-HO, respectively. The heme dissociation rate constants (k_{-H}) calculated from the average heme affinity (K_d) and the association rate constants (k_H) for PhuS or *pa*-HO were 0.036 and 0.066 s^{-1}, respectively. The rate of heme association of PhuS or *pa*-HO is similar to BSA (*20*) and comparable to that of the myoglobin (*21*), yet both PhuS and *pa*-HO have a markedly higher rate of heme dissociation compared to either myoglobin (8.4×10^{-7} s^{-1}) or BSA (3.2×10^{-4} s^{-1}), which would be a requirement of a heme-trafficking protein.

Heme Transfer Experiments. Kinetic traces for the heme transfer from PhuS to *pa*-HO-wt, mutants with altered regioselectivity (*pa*-HO-N19K/F117Y (*pa*-HO-DM), *pa*-HO-N19K/F117Y/K34N (DM-K34N), *pa*-HO-N19K/F117Y/K132A (DM-K132A)), the altered spin-state mutant (*pa*-HO-G125V), or BphO are shown in Figure 1. At pH 7.5, heme transfers from PhuS to *pa*-HO-wt, the *pa*-HO mutants, or BphO clearly display biphasic kinetics, and the time courses were therefore fit to a two-exponential expression. The average rates of the initial kinetic phases and the slow phase were 0.10 and 0.01 s^{-1} at 25 °C (pH 7.5), respectively. In contrast, the heme transfer from heme-PhuS to *pa*-HO-G125V displayed single-phase kinetics and was fit to a single-exponential expression with a k_{obs} of 0.1 s^{-1}. Therefore, we attribute the initial kinetic phase, k_1, to heme transfer from holo-PhuS to the respective HO proteins and the second phase rate, k_2, to change in heme spin change from LS to HS based on the results obtained with *pa*-HO-wt and *pa*-HO-G125V.

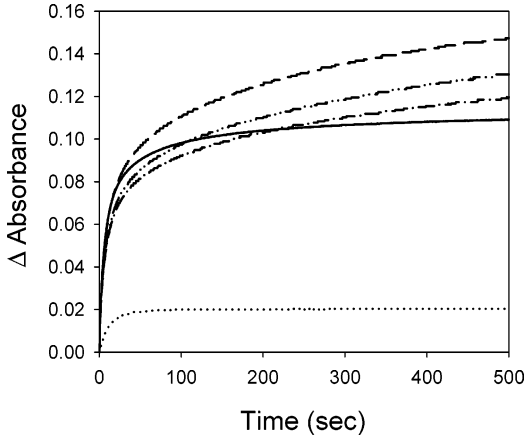

FIGURE 1: Time course of heme transfer from PhuS to *pa*-HO, paHO mutants, and BphO. (—) *pa*-HO (wt); (— —) *pa*-HO-N19K/F117Y(DM); (-•-) *pa*-HO-DM-K132A; (-••) *pa*-HO-DM-K34N; and (•••) BphO. Experiments were conducted with 10 μM PhuS, 30 μM *pa*-HO, and 30 μM BphO in 20 mM Tris-HCl, pH 7.5, at 25 °C, and time courses were measured at 405 nm.

The *pa*-HO-DM, DM-K34N, and DM-K132A were previously constructed and characterized to determine the role of specific surface residues in coordination of the heme propionates in stabilizing the heme for regioselective oxidative cleavage. These mutations have previously been shown to destabilize the heme within the protein such that it is in dynamic in-plane rotation between two seatings that yield an altered isomer pattern from that of the wild-type protein (*19*, *22*). Therefore, we would predict that such a destabilization would have an effect on the rate of heme transfer. Surprisingly, these mutants did not greatly alter or affect the overall rate of heme transfer, k_1, from PhuS when compared to the wild-type *pa*-HO, although a 3-fold decrease in the rate of the slow phase, k_2, was observed. These data suggest that amino acids that stabilize the heme within *pa*-HO have a minor influence on the overall heme transfer process.

The rate of heme transfer, k_1, from PhuS to the *pa*-HO mutants and BphO decreased by 3-fold going from pH 6.5 to 8.5 (Table 2). The increase in the rate of heme transfer to *pa*-HO and BphO is most likely due to the protonation of the proximal His side chain of PhuS, facilitating the loss (dissociation) of the Fe−His bond (*23*−*25*). Although, no correlation was observed between pH and the second phase of the reaction, at high pH, the slow phase, k_2, seemingly disappears, giving rise to a monophasic kinetics as shown in Figure 2. Previous spectroscopic characterization of both *pa*-HO and PhuS indicates that at neutral pH (pH 7.5) the heme−PhuS and heme−*pa*-HO complexes are 6-c LS and 6-c HS, respectively (*15*, *26*). However, above pH 8.0, an alkaline transition occurs whereby *pa*-HO switches from a 6-c HS to a 6-c LS system, indicating that a spin-transition may be involved in the transfer of heme from PhuS to *pa*-HO or BphO.

To test this hypothesis, experiments were conducted in the presence of 10 mM CN^-. Treatment of holo-PhuS with

Table 2: pH Dependence of the Rate Constant of Heme Transfer from PhuS to Selected *pa*-HO Mutants and BphO at 25 °C[a]

	rate of heme transfer (s^{-1}) at various pH[a]					
	6.5		7.5		8.5	
protein	k_1	k_2	k_1	k_2	k_1	k_2
pa-HO-wt	0.15 (1)	0.0074 (2)	0.10 (2)	0.0095 (1)	0.080 (1)	0.018 (1)
pa-HO-N19K/F117Y-(DM)	0.14 (1)	0.0048 (3)	0.10 (1)	0.0046 (2)	0.072 (1)	0.0085 (1)
DM-K34N	0.15 (1)	0.0059 (2)	0.11 (2)	0.0072 (1)	0.072 (1)	0.0062 (1)
DM-K132A	0.13 (1)	0.0051 (3)	0.10 (2)	0.0039 (1)	0.066 (1)	0.0050 (1)
pa-HO-G125V[b]	0.25 (2)	0.0083 (2)	0.10 (1)	-	0.081 (2)	-
BphO[b]	0.14 (2)	0.0062 (2)	0.10 (2)	0.0065 (3)	0.054 (1)	-

[a] Reactions were carried out in 20 mM Tris-HCl, at the corresponding pH, with 10 μM PhuS and 30 μM *pa*-HO/BphO. The reactions were fit to a two-exponential expression unless otherwise stated, and the standard deviations for the last significant figures are given in parentheses from the mean of at least three independent experiments. [b] Reaction were fit to a single-exponential expression.

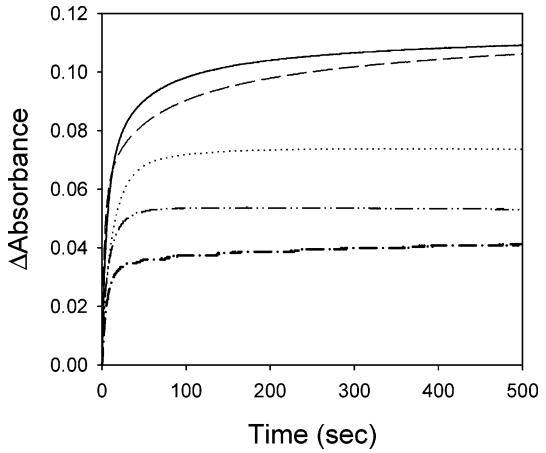

FIGURE 2: Time course of heme transfer from PhuS to *pa*-HO as a function of pH. (— —) pH 6.5; (—) 7.5; (···) 8.5; (—··) *pa*-HO-G125V, pH 7.5; and (—·—) *pa*-HO-wt with 10 mM KCN, pH 7.5. Experiments were conducted with 10 μM PhuS and 30 μM *pa*-HO in 20 mM Tris-HCl at the corresponding pH at 25 °C, and time courses were measured at 405 (for pH 6.5 and 7.5) and 410 nm (pH 8.5). Reaction conducted in the presence of KCN was monitored at 419 nm.

CN^- at pH 7.5 resulted in a shift of the Soret peak to 419 nm and a replacement of the distinct 528 and 560 nm peaks with a broadband at 530 nm, indicative of a low-spin CN^- complex. As shown in Figure 1, the absorbance time course for heme transfer from PhuS to *pa*-HO-wt, mutants, or BphO displays biphasic kinetics. Although, the rate of the fast phase, k_1 of 0.12 s^{-1}, was similar to the rate observed in the absence of CN^-, the rate of the slow phase, k_2 of 0.03 s^{-1}, was 3-fold slower compared to the rate observed for the slow phase in the absence of CN^-. Inhibition of k_2 by CN^- is indicative and supportive of the involvement of spin-change during the heme transfer.

Effect of Temperature on the Rate of Heme Transfer. The temperature dependence of heme transfer from PhuS to *pa*-HO, the *pa*-HO-mutants, or BphO at pH 7.5 is shown in Table 3. The rate of heme transfer increased with increasing temperature (Supporting Information; Table S1), and displayed linear and nonlinear Arrhenius plots for the fast-, k_1, and the slow-phase, k_2, of heme transfer from PhuS, respectively (Figure 3). A concave Arrhenius plot was obtained for the slow phase, k_2, of the reaction over the complete temperature range and was most likely due to composite of other rate constants or steps.

The activation energies at pH 7.5 for the heme transfer from PhuS to *pa*-HO-wt, *pa*-HO mutants, and BphO range from ~12 to 14 kcal/mol. The activation enthalpy and entropy ranged from 11.3 to 13.7 kcal/mol and −15 to −23 cal mol^{-1} K^{-1}, respectively (Table 3). The higher activation enthalpy of heme transfer to BphO by ~2 kcal/mol compared to *pa*-HO suggests that heme transfer from PhuS to *pa*-HO is more favorable than to BphO. However, the increase in enthalpy with BphO appears to be compensated by larger and favorable entropy, since the free energy of activation is similar for both proteins.

Table 3: Activation Parameters for Heme Transfer from PhuS to *pa*-HO-wt, *pa*-HO Mutants, and BphO in 20 mM Tris, pH 7.5

protein	E_a[a] (kcal/mol)	$\Delta H^{\ddagger a}$ (kcal/mol)	$\Delta S^{\ddagger a,b}$ (cal mol^{-1} K^{-1})	$\Delta G^{\ddagger}$ (kcal/mol)
pa-HO-wt	11.9	11.3	−22.9	18.2
pa-HO-N19K/F117Y-(DM)	12.0	11.4	−22.7	18.2
DM-K34N	12.9	12.3	−19.6	18.1
DM-K132A	12.2	11.6	−22.1	18.2
pa-HO-G125V	12.3	11.7	−22.1	18.3
BphO	14.3	13.7	−14.9	18.1

[a] The error limits for the apparent activation energy, enthalpy, and entropy reported were calculated to be approximately ±5%. [b] A temperature of 298 K was used in the ln Eyring pre-exponential term ($k_BT/\hbar$) when it was subtracted from the ln k axis intercept of the Arrhenius plot to determine the $\Delta S^{\ddagger}$ values.

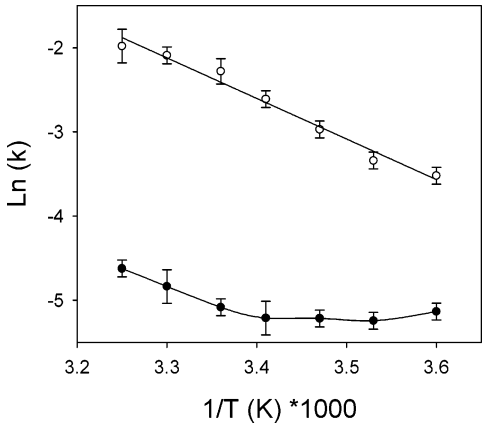

FIGURE 3: Arrhenius plot of heme transfer in the presence of 10 μM PhuS and 30 μM *pa*-HO in 20 mM Tris, pH 7.5. (○) Fast phase (k_1) and (●) slow phase (k_2).

The rates of heme transfer in the presence of CN^- and as a function of temperature are provided in the Supporting Information (Table S2). The temperature dependence of the activation parameters for heme transfer in the presence of CN^- are summarized in Table 4. The activation energy ranges from 12.3 to 17.2 kcal/mol for the *pa*-HO-wt and *pa*-HO mutants and 12.8 kcal/mol for BphO as calculated

Table 4: Activation Parameters for the Heme Transfer from PhuS to *pa*-HO-wt, *pa*-HO Mutants, and BphO in the Presence of 10 mM KCN in 20 mM Tris, pH 7.5

protein	E_a[a] (kcal/mol)	$\Delta H^{\ddagger a}$ (kcal/mol)	$\Delta S^{\ddagger a,b}$ (cal mol^{-1} K^{-1})	$\Delta G^{\ddagger}$ (kcal/mol)
pa-HO-wt	14.6	14.0	−13.7	18.1
pa-HO-N19K/F117Y-(DM)	17.2	16.6	−5.4	18.3
DM-K34N	12.3	11.7	−21.5	18.1
DM-K132A	14.4	13.8	−14.6	18.2
pa-HO-G125V	14.0	13.4	−16.3	18.2
BphO	12.8	12.2	−20.9	18.4

[a] The error limits for the apparent activation energy, enthalpy, and entropy reported were calculated to be approximately ±5%. [b] A temperature of 298 K was used in the ln Eyring pre-exponential term (k_BT/$\hbar$) when it was subtracted from the ln *k* axis intercept of the Arrhenius plot to determine the $\Delta S^{\ddagger}$ values.

from the slopes of the Arrhenius plots. The activation enthalpy for some of the *pa*-HO mutants drifts considerably from the WT protein and indicates that these amino acids must play an important role during the heme transfer process. The increase in the activation enthalpy appears to be compensated by favorable (or unfavorable) activation entropy. The high activation enthalpy obtained in the presence of CN^- (compared to without CN^-) of ∼12 kcal/mol suggests that *pa*-HO is not energetically competent to receive heme and/or stay in a low-spin-heme conformation at pH 7.5. On the other hand, transfer to BphO seems to be favored, and the transition state for the heme transfer is highly organized in the presence of CN^-. This may imply that the transfer to BphO as previously shown is not facilitated by a direct protein−protein interaction as is that of *pa*-HO, and the CN^- complex effectively destabilizes the holo-PhuS.

Heme Transfer from PhuS and pa-HO to Myoglobin or Bovine Serum Albumin (BSA). The rate of heme transfer from PhuS or *pa*-HO to myoglobin was examined as described in Materials and Methods. The time course for the transfer of heme from *pa*-HO or PhuS to myoglobin was fit to a single exponential (Figure 4). The pseudo-first-order rate constants for the heme dissociation from *pa*-HO and PhuS were (3.5 ± 0.1) × 10^{-3} and (3.8 ± 0.1) × 10^{-3} s^{-1}, respectively. The relative high rate of heme dissociation compared to that for myoglobin (Table 1) suggests that heme binds very weakly to PhuS and *pa*-HO, which would be expected for proteins that are involved in heme-trafficking and degradation, respectively. The 30-fold decrease in the rate of heme transfer from PhuS and *pa*-HO to myoglobin suggests that this process is solution-mediated as a result of the high affinity of myoglobin for heme and not via a direct protein interaction. To further support the above hypothesis, reactions were conducted with BSA, which has a similar rate of heme association and dissociation as *pa*-HO. Under standard experimental conditions, no heme transfer from PhuS to BSA occurred, as judged by UV−visible spectroscopy and size-exclusion chromatography (data not shown).

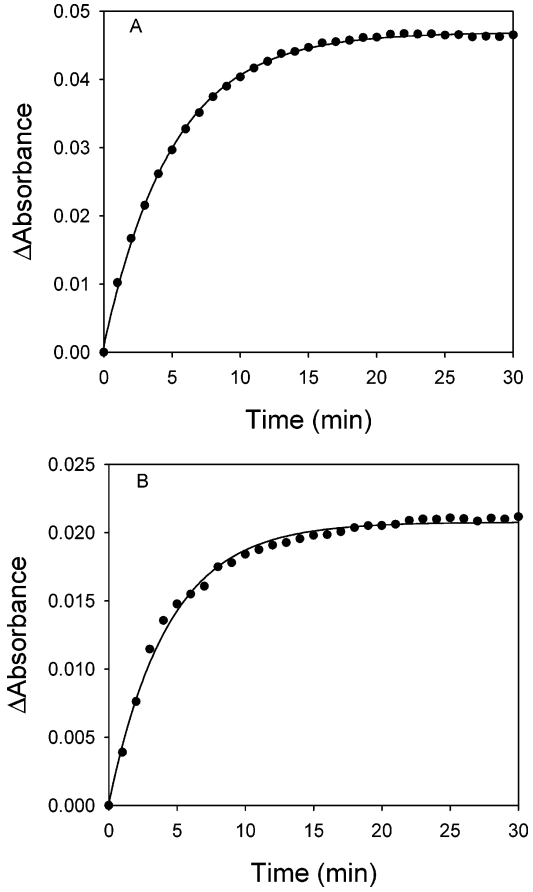

FIGURE 4: Heme transfer from (A) *pa*-HO and (B) PhuS to myoglobin. Reactions were conducted in 20 mM Tris-HCl, pH 7.5, at 25 °C with 2 μM *pa*-HO or PhuS and 12 μM myoglobin, and the time course was measured at 408 nm.

DISCUSSION

It has previously been shown that the PhuS homologue HemS is required for efficient heme utilization in *Y. entercolitica* (*14*). We therefore hypothesized that heme as it enters the cell is sequestered by PhuS which serves as a heme carrier that delivers heme to the iron-regulated heme oxygenase, *pa*-HO. Oxidative ring opening of the porphyrin by *pa*-HO then releases iron for further utilization by the cell. Recently, we provided evidence for this hypothesis via a comprehensive *in vitro* biochemical and spectroscopic analysis of the heme-PhuS complex and its role as a specific heme chaperone to *pa*-HO (*15*). The possibility of nonspecific solution-mediated heme transfer was judged unlikely since similar kinetics were observed under excess amounts of *pa*-HO. Furthermore, a similar product distribution and regioselectivity was observed on coupled oxidation of either *pa*-HO alone or Phus/*pa*-HO, which suggests that heme transfer from PhuS to *pa*-HO is specific and most likely driven by direct protein−protein interaction (data not shown). The inability of apo-PhuS to acquire heme from holo-*pa*-HO also excluded the possibility of reverse heme transfer and confirmed that the transfer is unidirectional and facilitated by direct protein−protein interaction, which was further confirmed by surface plasmon resonance (SPR) (*15*).

In contrast, heme transfer from holo-PhuS to BphO is reversible indicating that the affinity of heme-PhuS for BphO is low and the absorbance spectra recorded during transfer do not exhibit behavior consistent with complete transfer of the heme. This behavior is indicative of a dissociative heme transfer mechanism that involves release of the heme into solution which was confirmed by the lack of a protein−protein interaction as judged by SPR. Therefore, in contrast to the mechanistically specific transfer of heme from PhuS to *pa*-HO, the transfer of heme between PhuS and BphO is most likely governed by their relative intrinsic affinities for heme.

Scheme 1

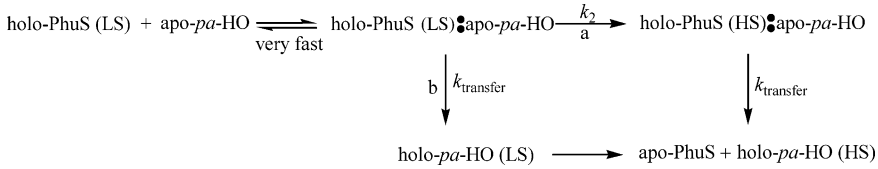

The rapid and unidirectional transfer of heme from PhuS to *pa*-HO, and the high affinity of PhuS for *pa*-HO compared to BphO, supports the hypothesis that PhuS acts as a heme-chaperone to *pa*-HO. To further substantiate this, and to show that heme transfer is not governed by the intrinsic heme-affinity of the respective proteins, transfer studies from holo-PhuS to *pa*-HO were conducted in parallel with myoglobin and BSA, which have a higher heme affinity than either *pa*-HO or PhuS. If the intrinsic heme affinity of a protein is the primary factor, then the rate of heme transfer from holo-PhuS to BSA and apomyoglobin should have been similar or decidedly faster, respectively, than that of transfer to *pa*-HO. However, the lack of heme transfer observed for BSA, and a slow rate for myoglobin, indicates that heme transfer to *pa*-HO is independent of the heme affinity of the protein, and other factors such as a protein−protein interaction may be involved in triggering heme transfer.

The rate of heme transfer from PhuS to *pa*-HO and the *pa*-HO mutants is similar regardless of pH (Table 2), although the increase in the rate of heme transfer at acidic pH may be due to protonation of the proximal histidine (*23*−*25*). However, the rate of heme transfer appears to be temperature-dependent with increased rates at higher temperatures. The increase in the activation energy for heme transfer from holo-PhuS to the *pa*-HO mutants relative to the native protein is most likely due to the loss of favorable binding or interaction between PhuS and *pa*-HO. The *pa*-HO mutants introduced heme propionate interactions required for α-regioselective specificity (*pa*-HO-N19K/F117Y) as in other characterized HO enzymes and additionally removed residues that stabilize the δ-regioselective heme seating (*pa*-HO-N19K/F117Y/K132A and *pa*-HO-N19K/F117Y/K34A) (*19*). In addition, these amino acid replacements are located on the heme binding face of *pa*-HO and, as well as stabilizing the bound heme, are located such that in the apo-*pa*-HO they may provide additional electrostatic or hydrogen-bonding interactions with the holo-PhuS (*22*). Furthermore, reactions conducted in the presence of 200 mM sodium chloride inhibited the process by ∼40% (data not shown), suggesting that electrostatic interactions may play a significant role during heme transfer from PhuS to *pa*-HO. The low activation of entropy of the wild-type *pa*-HO suggests that the transition state is highly ordered, and this stabilization could be provided in the form of a protein−protein interaction, which is consistent with the gain in entropy observed for the *pa*-HO mutants and BphO. However, an exact interpretation of these effects will require a more extensive study with a larger set of mutants at these and other positions in and around the heme pocket of both PhuS and *pa*-HO.

Previous observations suggested that at neutral pH the heme−PhuS and heme−*pa*-HO complexes are 6-c LS and 6-c HS, respectively (*15*, *19*). Therefore, changes in both the spin-state and axial heme coordination must occur during the transfer reaction. These transformations may be driven by the free energy yield of protein−protein complexation, thereby triggering the transfer reaction. The ready accessibility of both the 6-c LS and 6-c HS spin states in the heme−PhuS complex suggests this could be a feasible triggering mechanism for heme transfer. In the presence of a strong ligand such as CN^-, both holo-PhuS and holo-*pa*-HO are 6-c LS, as expected. Therefore, reactions conducted in the presence of CN^- should have exhibited first-order kinetics, since heme transfer from PhuS to *pa*-HO should not involve spin change prior (in PhuS) or after (*pa*-HO) the heme transfer step. However, the biphasic kinetics observed in the presence of CN^- suggests that heme-spin change must occur within PhuS prior to the heme transfer step.

Thermodynamic parameters obtained for the reaction conducted in the presence and absence CN^- indicate that enthalpy and entropy greatly influence heme transfer. Although the free energy of activation $\Delta G^{\ddagger}$ values for the heme transfer in the presence or absence of CN^- are similar, $\Delta H^{\ddagger}$ for heme transfer is higher, ∼2 kcal/mol, in the presence of CN^-, while $\Delta S^{\ddagger}$ is lower ∼8 cal mol^{-1} K^{-1} in the absence of CN^-. Thus, the equal free energies of these two transition states are due to the compensating differences in enthalpy and entropy. The small negative relative activation enthalpy, $\Delta\Delta H^{\ddagger}$, determined for heme transfer from holo-PhuS to *pa*-HO-wt or the *pa*-HO mutants, suggests that the heme transfer in the absence of CN^- is favored by the activation enthalpy compared to the reaction in the presence of CN^-. However, the relative activation entropy, $\Delta\Delta S^{\ddagger}$, for the heme transfer is negative, suggesting that the transition state for the heme transfer in the absence of CN^- is much more ordered, organized, and entropically unfavorable in comparison to that of in the presence of CN^-. These results suggest that the transition states of the reaction in the presence and absence of CN^- are structurally different, and consequently, the gain of entropy in the CN^--dependent reaction could be attributed to major changes in conformation of the protein and/or the spin state of the heme prior to the transfer. In addition, the high activation enthalpy associated with the CN^- reaction suggests that PhuS is not primed to transfer heme in the low-spin state and must undergo a spin transition prior to heme transfer, as shown in Scheme 1, pathway a. This pathway is further supported by the fact that reactions conducted in the presence of CN^- and at pH 8.5 should have behaved similarly to the *pa*-HO-G125V mutant, since both holo-PhuS and holo-*pa*-HO are 6-c LS. However, the biphasic kinetics observed in the above-mentioned reactions is suggestive of a spin change occurring within the heme−PhuS complex, and this could be the triggering step that leads to heme transfer.

Since k_1 and k_2 are associated to the rate of heme transfer and spin change respectively, then the formation of the PhuS(HS):*pa*-HO complex is rate-determining ($k_2 < k_1$) and first-order kinetics should have been observed if only pathway a is operative. However, the presence of the biphasic kinetics

can be rationalized if an alternate pathway is also operative which involves a direct transfer of heme from PhuS to *pa*-HO (Scheme 1, pathway b). The scenario of both pathways being operative is plausible, whereby pathway a shows a first-order reaction with a rate constant of k_2, and pathway b would comprise a first-order transfer of heme from holo-PhuS to *pa*-HO, producing a transient holo-*pa*-HO (LS) species, followed by conversion to a high-spin state within *pa*-HO. The concave Arrhenius plot for k_2 is consistent with the assumption that this pathway consists of at least two kinetic steps. This model explains the observed results with *pa*-HO-G125V, 6-c LS, which has a similar rate of heme transfer, k_1 of $\sim$0.1 s^{-1}, as the wild-type protein and supports the notion that spin transition could occur within *pa*-HO as well as suggests that heme spin crossover may not be required prior to the heme transfer step. Although, the data does not conclusively support the possibility of either or both pathways being operative, it clearly shows that spin change must be involved during the heme transfer from holo-PhuS to apo-*pa*-HO.

Concluding Remarks. Taken together these studies indicate that the cytoplasmic heme binding protein PhuS acts as a specific heme-chaperone to the iron-regulated *pa*-HO, and the biphasic behavior associated with heme transfer leads us to propose a model which involves a dual pathway for heme transfer. On the basis of the magnitudes of the activation parameters for the reactions conducted in the presence and absence of CN^-, we propose that spin change should occur within the heme−PhuS complex, and this is the triggering step that leads to heme transfer. Results from *pa*-HO-G125V suggest that spin change may not be required and is supportive of a pathway which involves a direct heme transfer from PhuS to *pa*-HO. While the current data support the requirement of a spin-state crossover for heme transfer from PhuS to *pa*-HO, the specific step in the reaction where this transition occurs will require further experimental analysis.

SUPPORTING INFORMATION AVAILABLE

Temperature dependence of the rate constant of heme transfer from PhuS to *pa*-HO-wt, *pa*-HO mutants, and BphO; temperature dependence of the rate constant of heme transfer from PhuS to *pa*-HO-wt, *pa*-HO mutants, and BphO in the presence of 10 mM KCN. This material is available free of charge via the Internet at http://pubs.acs.org.

REFERENCES

1. Wandersman, C., and Stojiljkovic, I. (2000) Bacterial heme sources: the role of heme, hemoprotein receptors and hemophores, *Curr. Opin. Microbiol. 3*, 215−220.
2. Wandersman, C., and Delepelaire, P. (2004) Bacterial iron sources: from siderophores to hemophores, *Annu. Rev. Microbiol. 58*, 611−647.
3. Henderson, D. P., and Payne, S. M. (1993) Cloning and characterization of the *Vibrio cholerae* genes encoding the utilization of iron from haemin and haemoglobin, *Mol. Microbiol. 7*, 461−469.
4. Mills, M., and Payne, S. M. (1995) Genetics and regulation of heme iron transport in *Shigella dysenteriae* and detection of an analogous system in *Escherichia coli* O157:H7, *J. Bacteriol. 177*, 3004−3009.
5. O'Malley, S. M., Mouton, S. L., Occhino, D. A., Deanda, M. T., Rashidi, J. R., Fuson, K. L., Rashidi, C. E., Mora, M. Y., Payne, S. M., and Henderson, D. P. (1999) Comparison of the heme iron utilization systems of pathogenic Vibrios, *J. Bacteriol. 181*, 3594−3598.
6. Drazek, E. S., Hammack, C. A., and Schmitt, M. P. (2000) *Corynebacterium diphtheriae* genes required for acquisition of iron from haemin and haemoglobin are homologous to ABC haemin transporters, *Mol. Microbiol. 36*, 68−84.
7. Ochsner, U. A., Johnson, Z., and Vasil, M. L. (2000) Genetics and regulation of two distinct haem-uptake systems, phu and has, in *Pseudomonas aeruginosa*, *Microbiology 146*, 185−198.
8. Mey, A. R., and Payne, S. M. (2001) Haem utilization in *Vibrio cholerae* involves multiple TonB-dependent haem receptors, *Mol. Microbiol. 42*, 835−849.
9. Wilks, A. (2002) Heme oxygenase: evolution, structure, and mechanism. *Antioxid. Redox Signaling 4*, 603−614.
10. Costerton, J. W. (2001) Cystic fibrosis pathogenesis and the role of biofilms in persistent infection, *Trends Microbiol. 9*, 50−52.
11. Currie, A. J., Speert, D. P., and Davidson, D. J. (2003) *Pseudomonas aeruginosa*: role in the pathogenesis of the CF lung lesion, *Semin. Respir. Crit. Care Med. 24*, 671−680.
12. Elkin, S., and Geddes, D. (2003) Pseudomonal infection in cystic fibrosis: the battle continues, *Exp. Rev. Anti. Infect. Ther. 1*, 609−618.
13. Letoffe, S., Ghigo, J. M., and Wandersman, C. (1994) Secretion of the Serratia marcescens HasA protein by an ABC transporter, *J. Bacteriol. 176*, 5372−5377.
14. Stojiljkovic, I., and Hantke, K. (1992) Hemin uptake system of *Yersinia enterocolitica*: similarities with other TonB-dependent systems in gram-negative bacteria, *EMBO J. 11*, 4359−4367.
15. Lansky, I. B., Lukat-Rodgers, G. S., Block, D., Rodgers, K. R., Ratliff, M., and Wilks, A. (2006) The cytoplasmic heme-binding protein (PhuS) from the heme uptake system of *Pseudomonas aeruginosa* is an intracellular heme-trafficking protein to the delta -regioselective heme oxygenase, *J. Biol. Chem. 281*, 13652−13662.
16. Tasler, R., Moises, T., and Frankenberg-Dinkel, N. (2005) Biochemical and spectroscopic characterization of the bacterial phytochrome of *Pseudomonas aeruginosa*, *FEBS J. 272*, 1927−1936.
17. Wegele, R., Tasler, R., Zeng, Y., Rivera, M., and Frankenberg-Dinkel, N. (2004) The heme oxygenase(s)-phytochrome system of *Pseudomonas aeruginosa*, *J. Biol. Chem.* 279, 45791−45802.
18. Ascoli, F., Fanelli, M. R., and Antonini, E. (1981) Preparation and properties of apohemoglobin and reconstituted hemoglobins. *Methods Enzymol. 76*, 72−87.
19. Caignan, G. A., Deshmukh, R., Wilks, A., Zeng, Y., Huang, H. W., Moenne-Loccoz, P., Bunce, R. A., Eastman, M. A., and Rivera, M. (2002) Oxidation of heme to beta- and delta-biliverdin by *Pseudomonas aeruginosa* heme oxygenase as a consequence of an unusual seating of the heme, *J. Am. Chem. Soc. 124*, 14879−14892.
20. Gattoni, M., Boffi, A., Sarti, P., and Chiancone, E. (1996) Stability of the heme-globin linkage in ab dimers and isolated chains of human hemoglobin. A study of the heme transfer reaction from the immobilized proteins to albumin, *J. Biol. Chem. 271*, 10130−10136.
21. Hargrove, M. S., Barrick, D., and Olson, J. S. (1996) The association rate constant for heme binding to globin is independent of protein structure, *Biochemistry. 35*, 11293−11299.
22. Friedman, J., Lad, L., Li, H., Wilks, A., and Poulos, T. L. (2004) Structural basis for novel delta-regioselective heme oxygenation in the opportunistic pathogen *Pseudomonas aeruginosa*, *Biochemistry 43*, 5239−5245.
23. Giacometti, G. M., Traylor, T. G., Ascenzi, P., Brunori, M., and Antonini, E. (1977) Reactivity of ferrous myoglobin at low pH, *J. Biol. Chem. 252*, 7447−748.
24. Coletta, M., Ascenzi, P., Traylor, T. G., and Brunori, M. (1985) Kinetics of carbon monoxide binding to monomeric hemoproteins. Role of the proximal histidine, *J. Biol. Chem. 260*, 4151−4155.
25. Hargrove, M. S., Singleton, E. W., Quillin, M. L., Ortiz, L. A., Phillips, G. N., Jr., Olson, J. S., and Mathews, A. J. (1994) His64-(E7) -> Tyr apomyoglobin as a reagent for measuring rates of hemin dissociation, *J. Biol. Chem. 269*, 4207−4214.
26. Caignan, G. A., Deshmukh, R., Zeng, Y., Wilks, A., Bunce, R. A., and Rivera, M. (2003) The hydroxide complex of *Pseudo-*

monas aeruginosa heme oxygenase as a model of the low-spin iron(III) hydroperoxide intermediate in heme catabolism: 13C NMR spectroscopic studies suggest the active participation of the heme in macrocycle hydroxylation, *J. Am. Chem. Soc. 125*, 11842−11852.

27. Rodriguez, J. C., Wilks, A., and Rivera, M. (2006) Backbone NMR assignments and H/D exchange studies on the ferric azide- and cyanide-inhibited forms of *Pseudomonas aeruginosa* heme oxygenase, *Biochemistry 45*, 4578−4592.

BI060980L